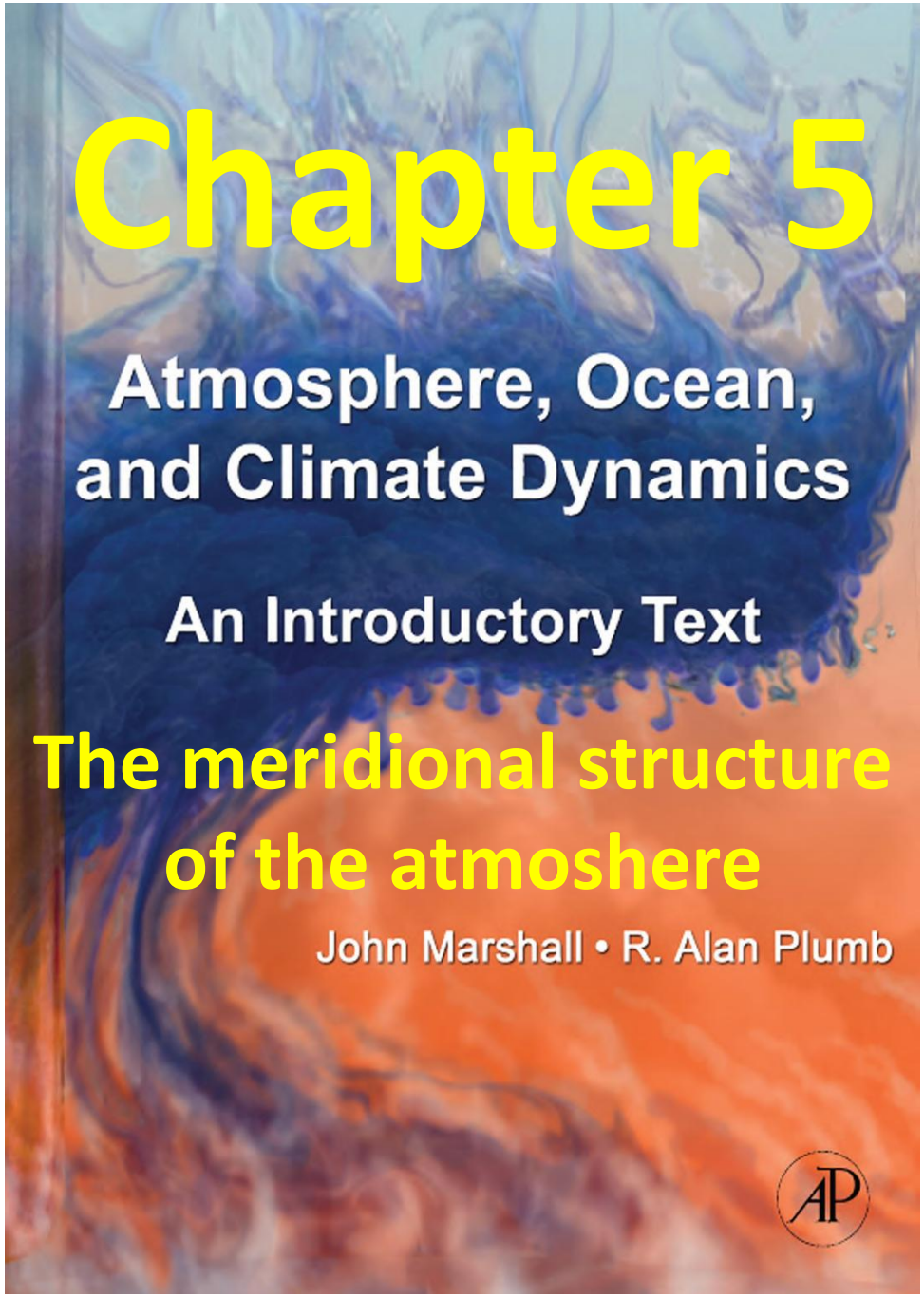
Chapter 5
Atmosphere, Ocean, and Climate Dynamics
An Introductory Text
The meridional structure of the atmoshere
John Marshall • R. Alan Plumb
AP

Latitudinal distribution
Incoming radiation

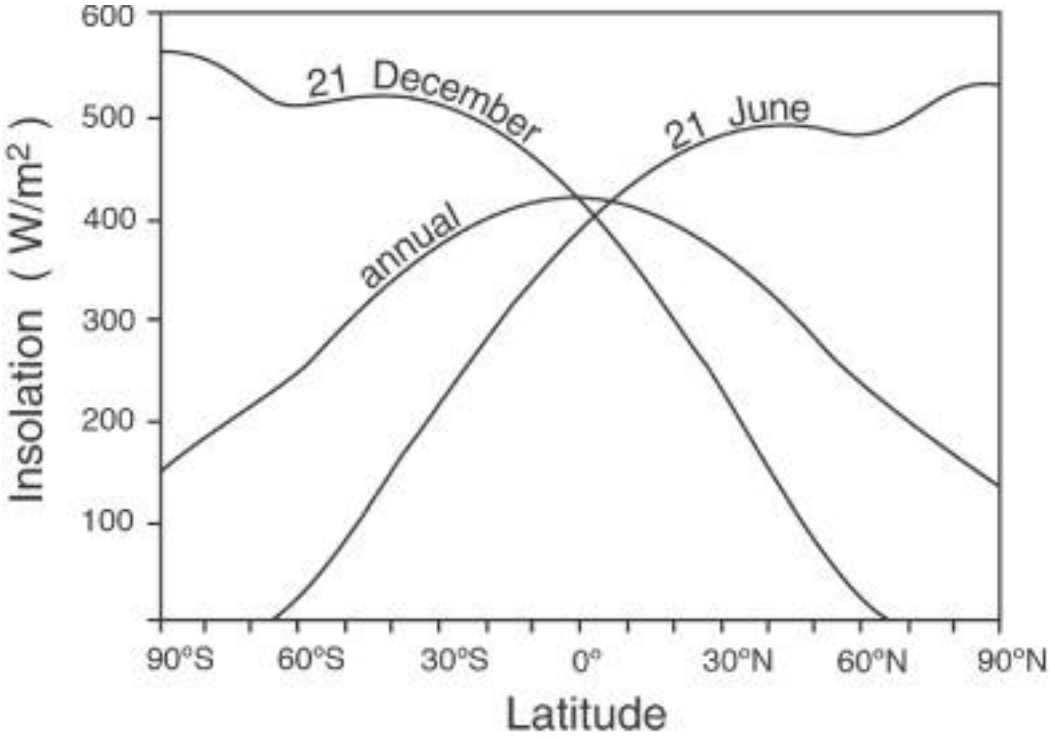

Figure 5.2: Distribution of annual mean and solstice (see Fig. 5.4) incoming solar radiation. The slight dip in the distribution at, for example, the winter solstice (December 21st) in the southern hemisphere corresponds to the edge of the polar day.

Latitudinal distribution
Incoming radiation

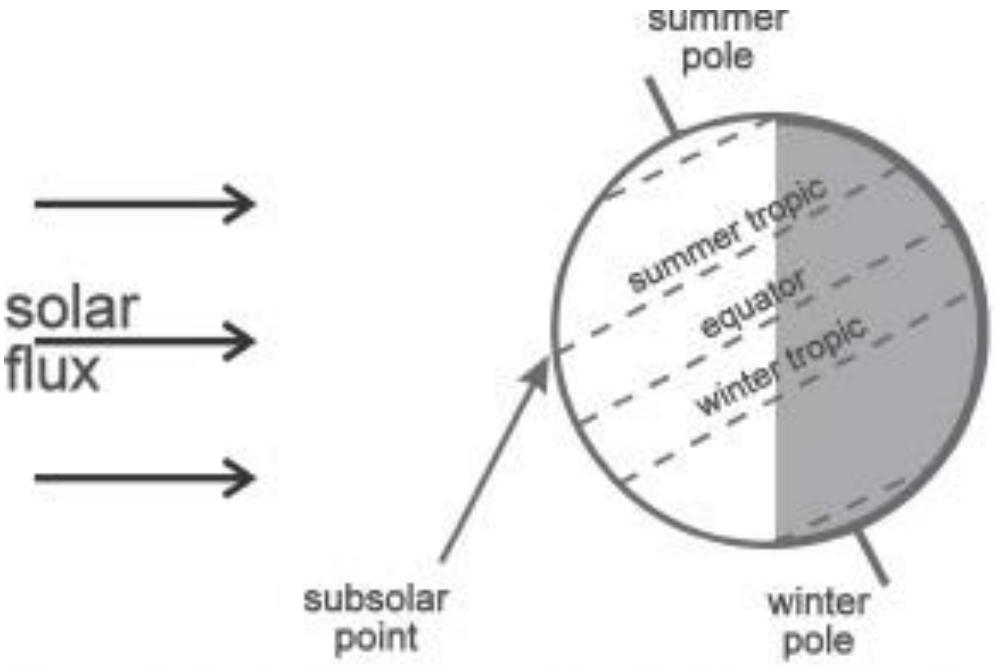

Figure 5.3: At the present time in history, the Earth's axis tilts at 23.5^3 and points towards the North Star. We sketch the incoming solar radiation at summer solstice when the Earth is tilted toward the Sun

Latitudinal and seasonal distribution
Incoming radiation

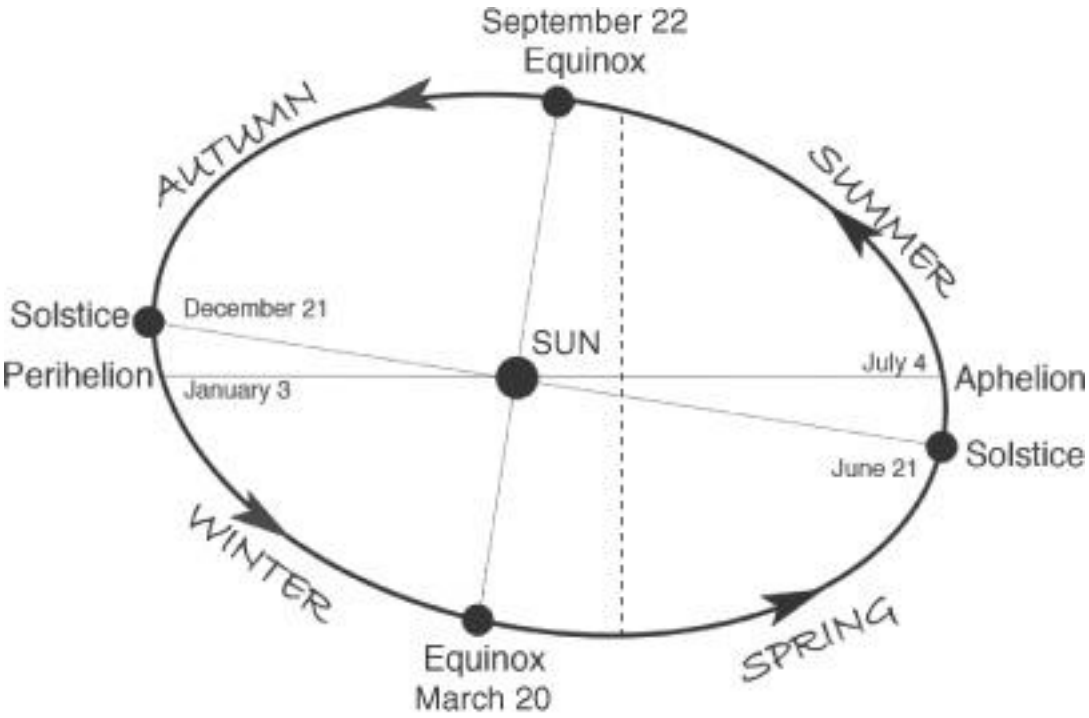

Figure 5.4: Earth describes an elliptical orbit around the Sun, greatly exaggerated in the figure. The longest (shortest) day occurs at the summer (winter) solstice when the Earth's spin axis points toward (away from) the Sun. The Earth is farthest from (closest to) the Sun at aphelion (perihelion). The seasons are labelled for the northern hemisphere.

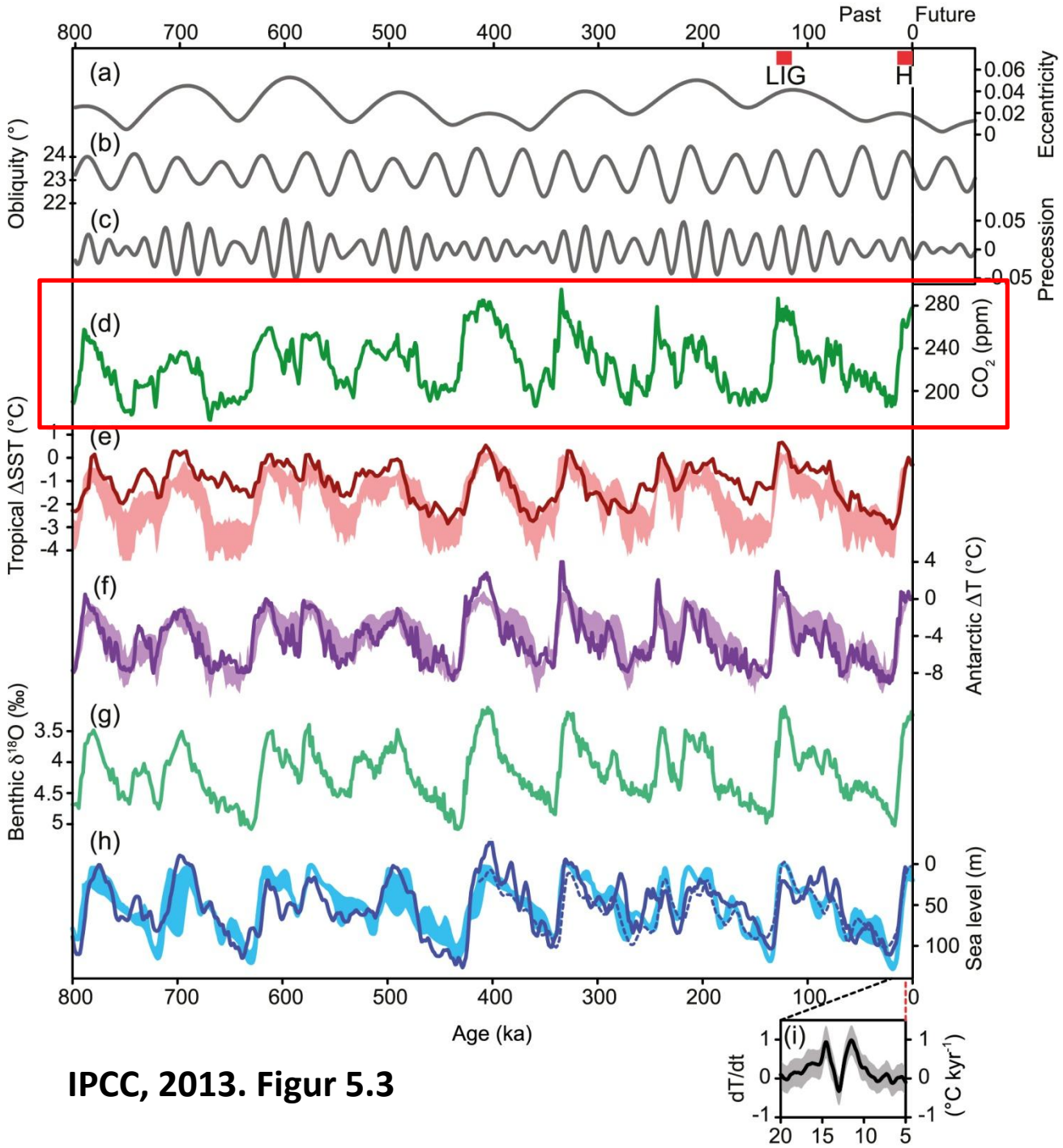

IPCC, 2013. Figur 5.3

Pådriv og responser i klimasystemet

Her: Temperaturendringen kommer først

➔CO_2 endringer følger

De siste 150 år: CO_2 økning skyldes hovedsakelig bruk av fossilt brennstoff.

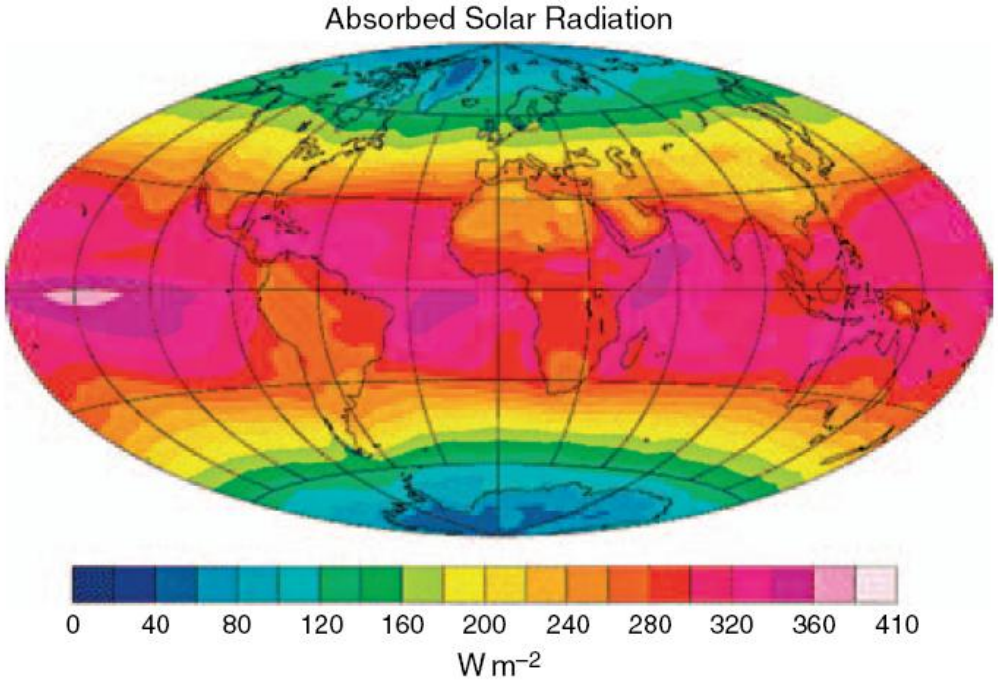

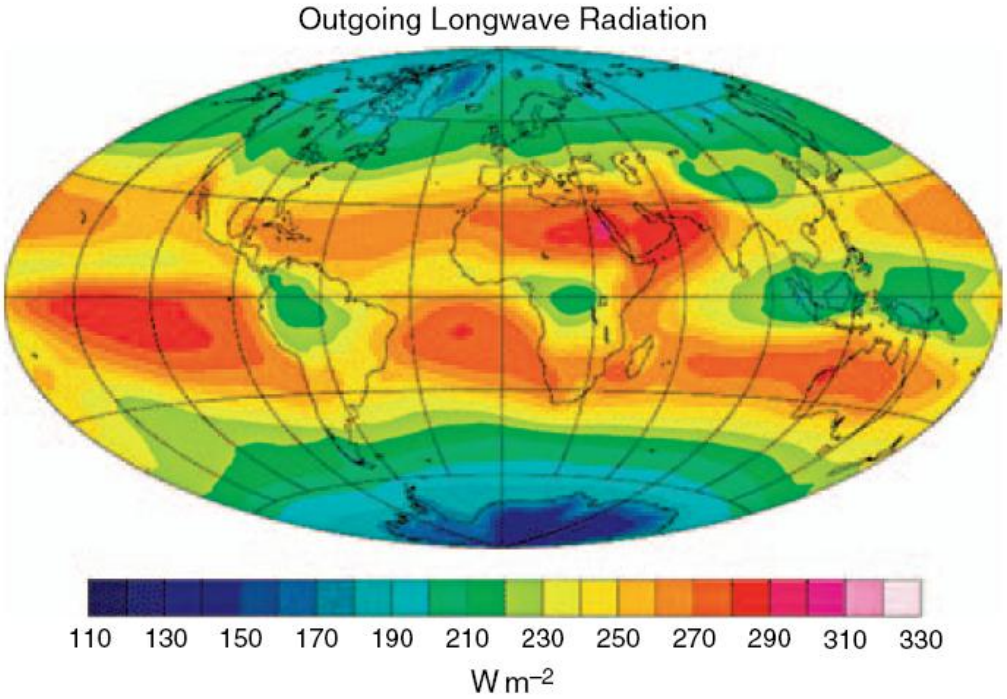

Årlig midlete netto strålingsflukser ved TOA.

Årlig midlet netto (kort- og langbølget)

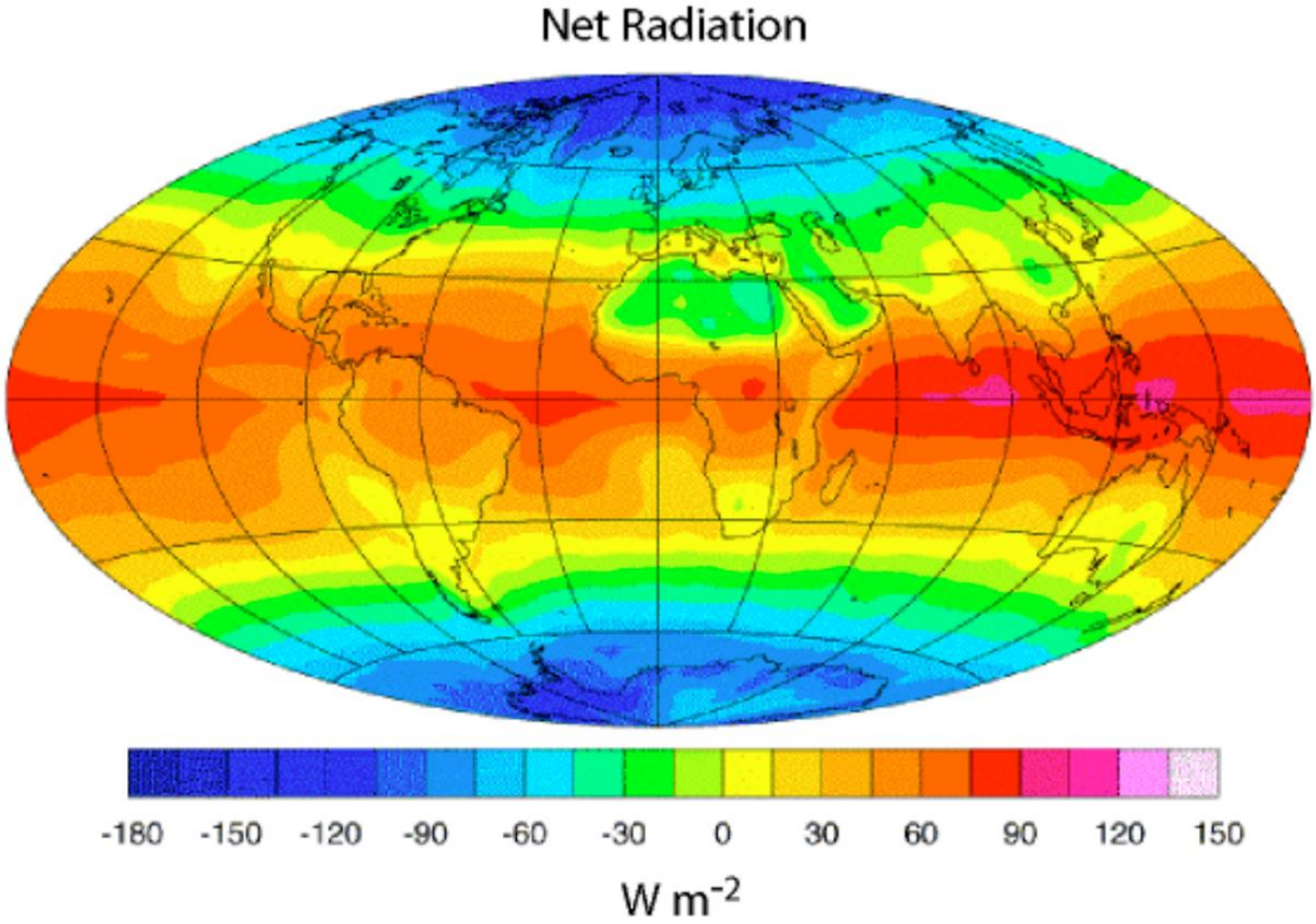

Latitudinal distribution
Incoming, outgoing and net radiation

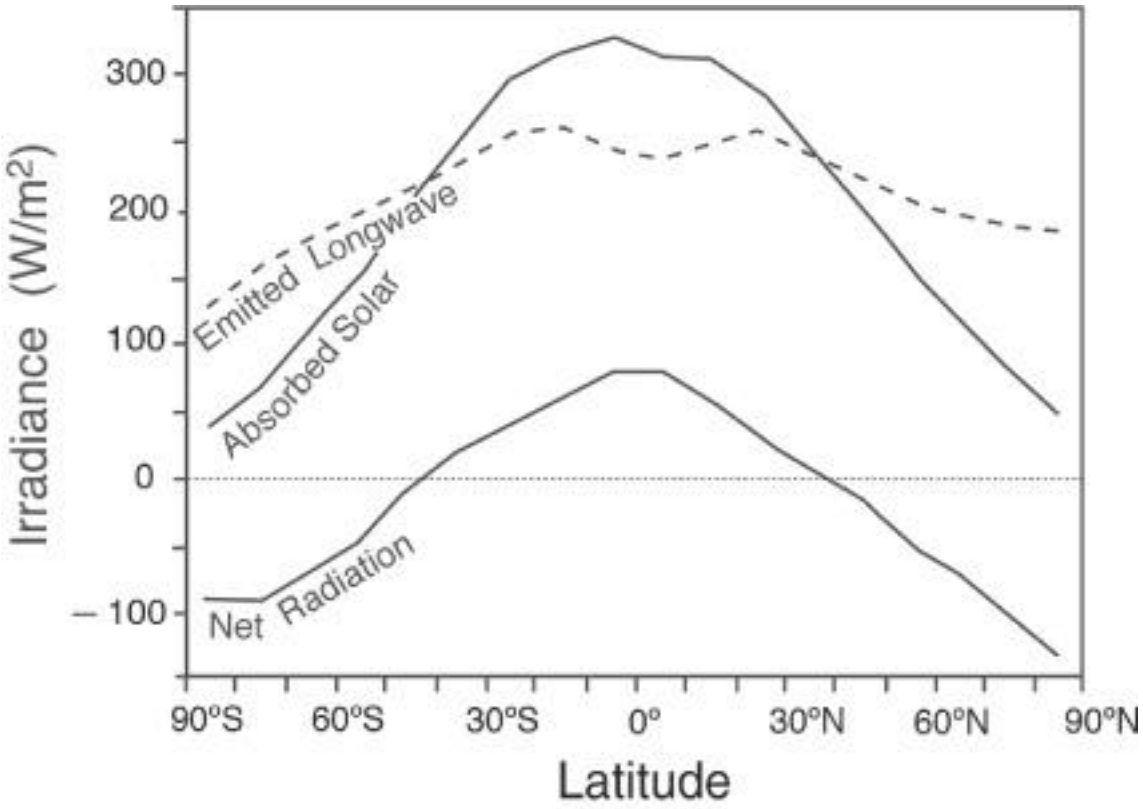

Figure 5.5: Annual mean absorbed solar radiation, emitted long-wave radiation, and net radiation, the sum of the two. The slight dip in emitted long-wave radiation at the equator is due to radiation from the (cold) tops of deep convecting clouds, as can be seen in Fig. 4.26.

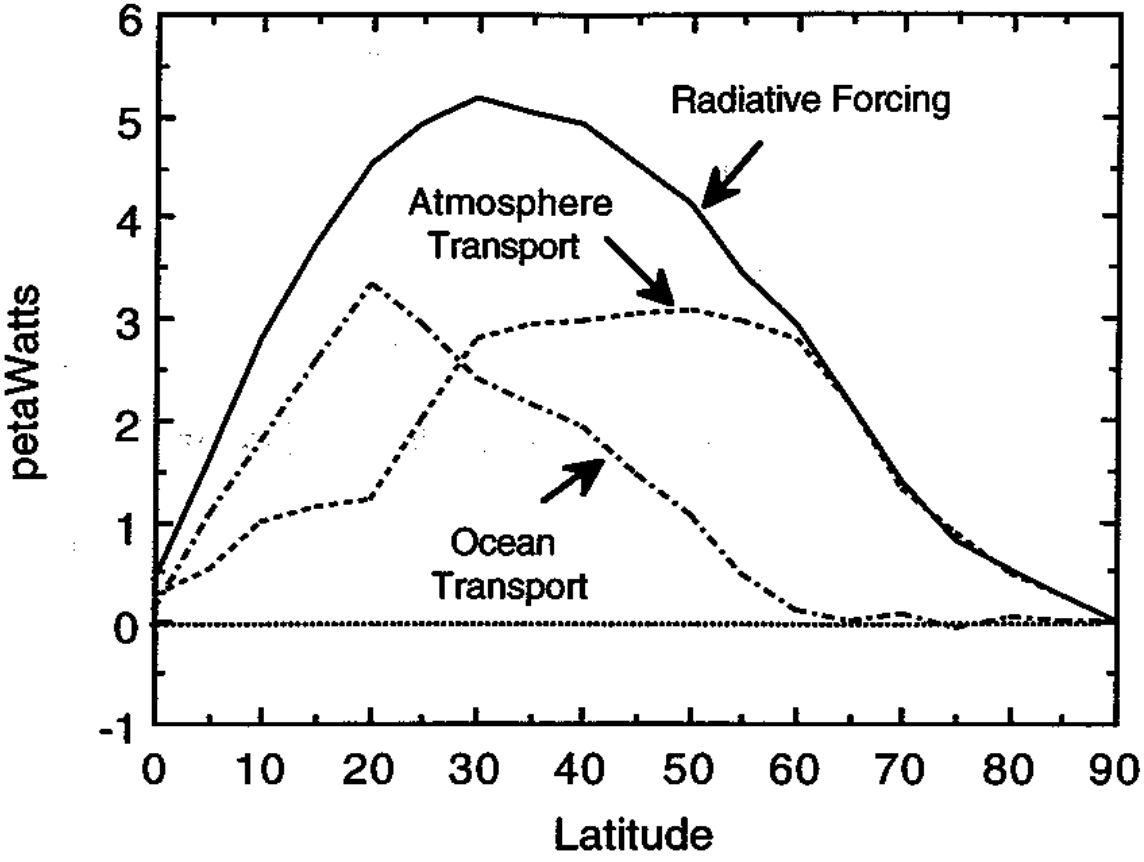

Fig. 2.14 Meridional transport of energy for annual-mean conditions. Net radiation and atmospheric transport are estimated from observations; ocean transport is calculated as a residual in the energy balance. [Adapted from Vonder Haar and Oort (1973). Used with permission from the American Meteorological Society.]

Meridional northward transport needed to balance

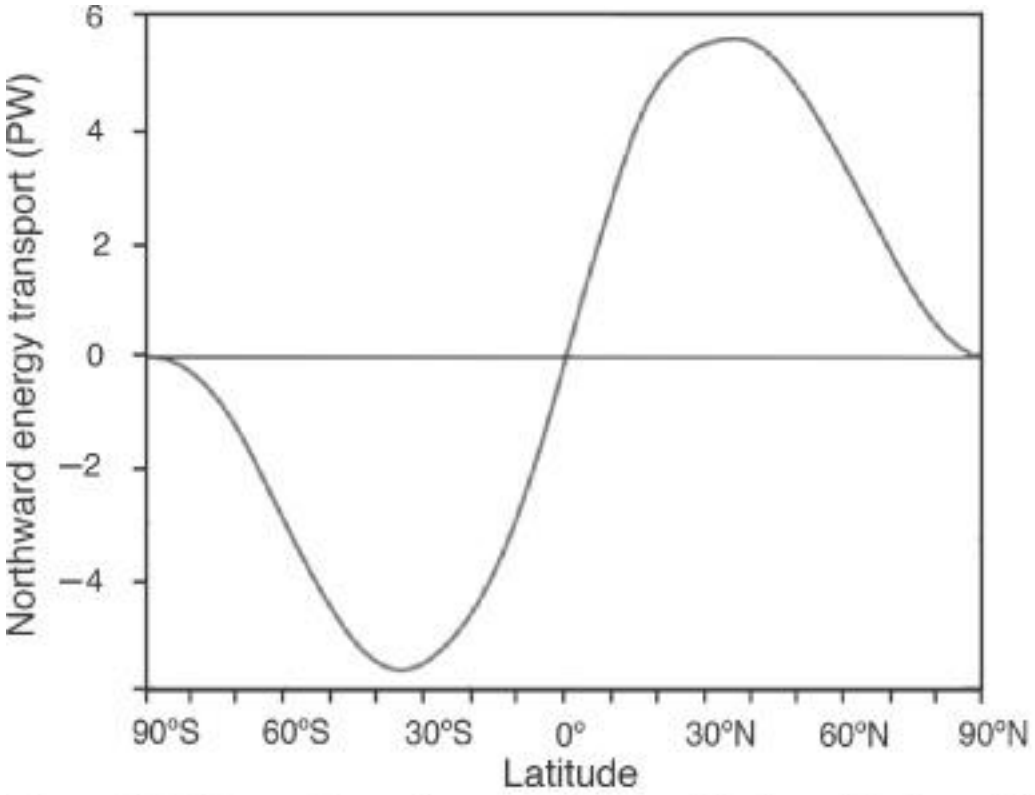

Figure 5.6: The northward energy transport deduced by top of the atmosphere measurements of incoming and outgoing solar and terrestrial radiation from the ERBE satellite. The units are in $PW = 10^{15}$W (see Trenberth and Caron, 2001). This curve is deduced by integrating the "net radiation" plotted in Fig. 5.5 meridionally. See Chapter 11 for a more detailed discussion.

Temperature in the tropsophere

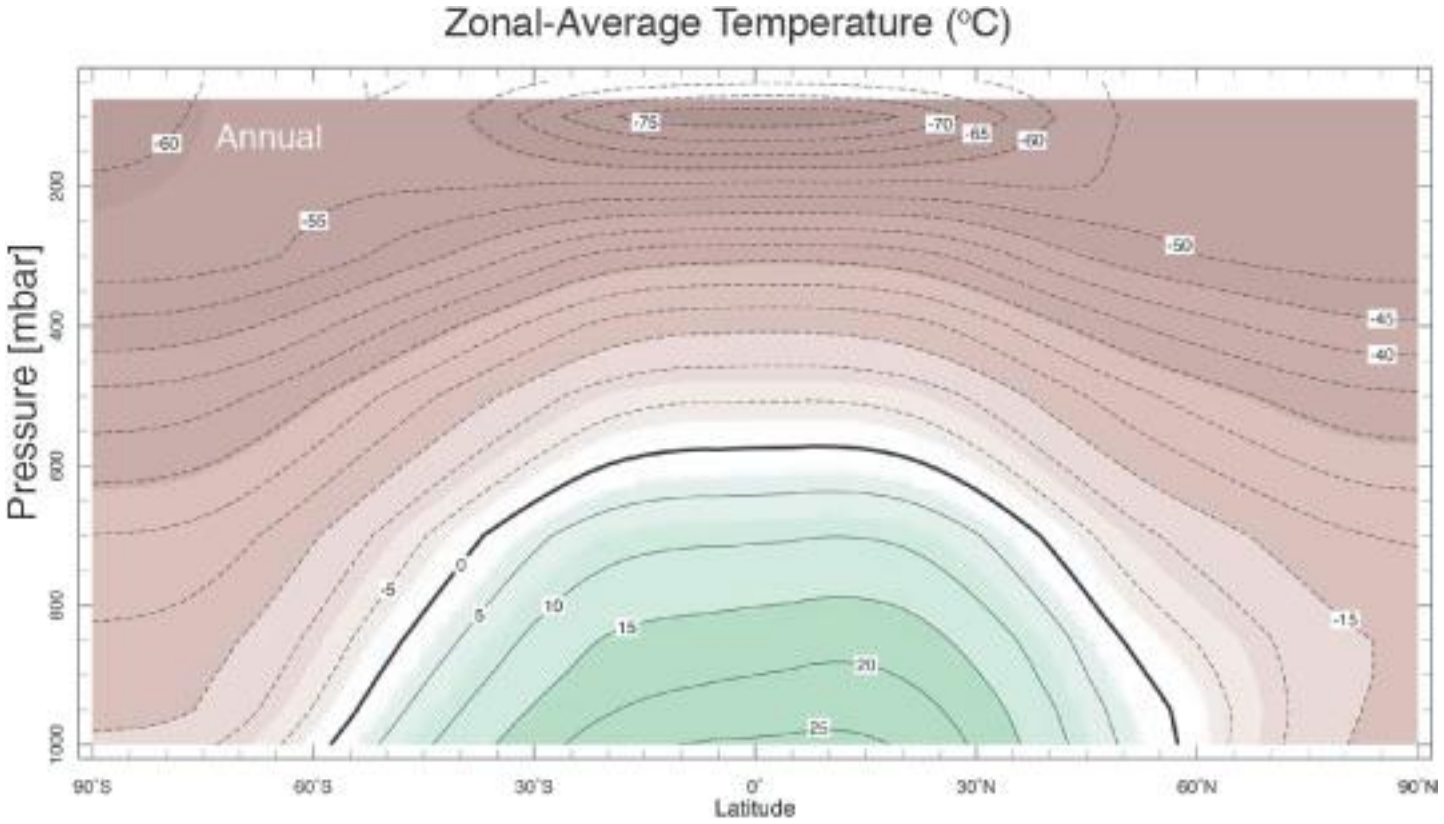

Figure 5.7: The zonally averaged annual-mean temperature in °C.

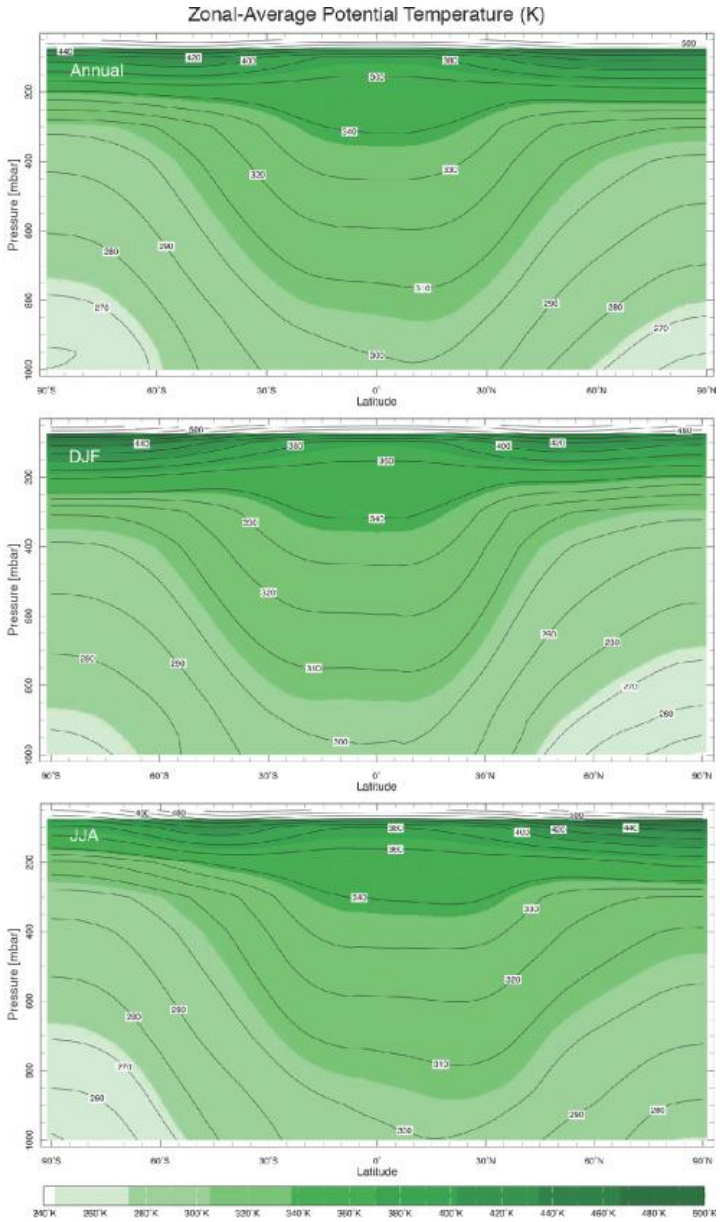

Figure 5.8: The zonally averaged potential temperature in (top) the annual mean, averaged over (middle) December, January, and February (DJF), and (bottom) June, July, and August (JJA).

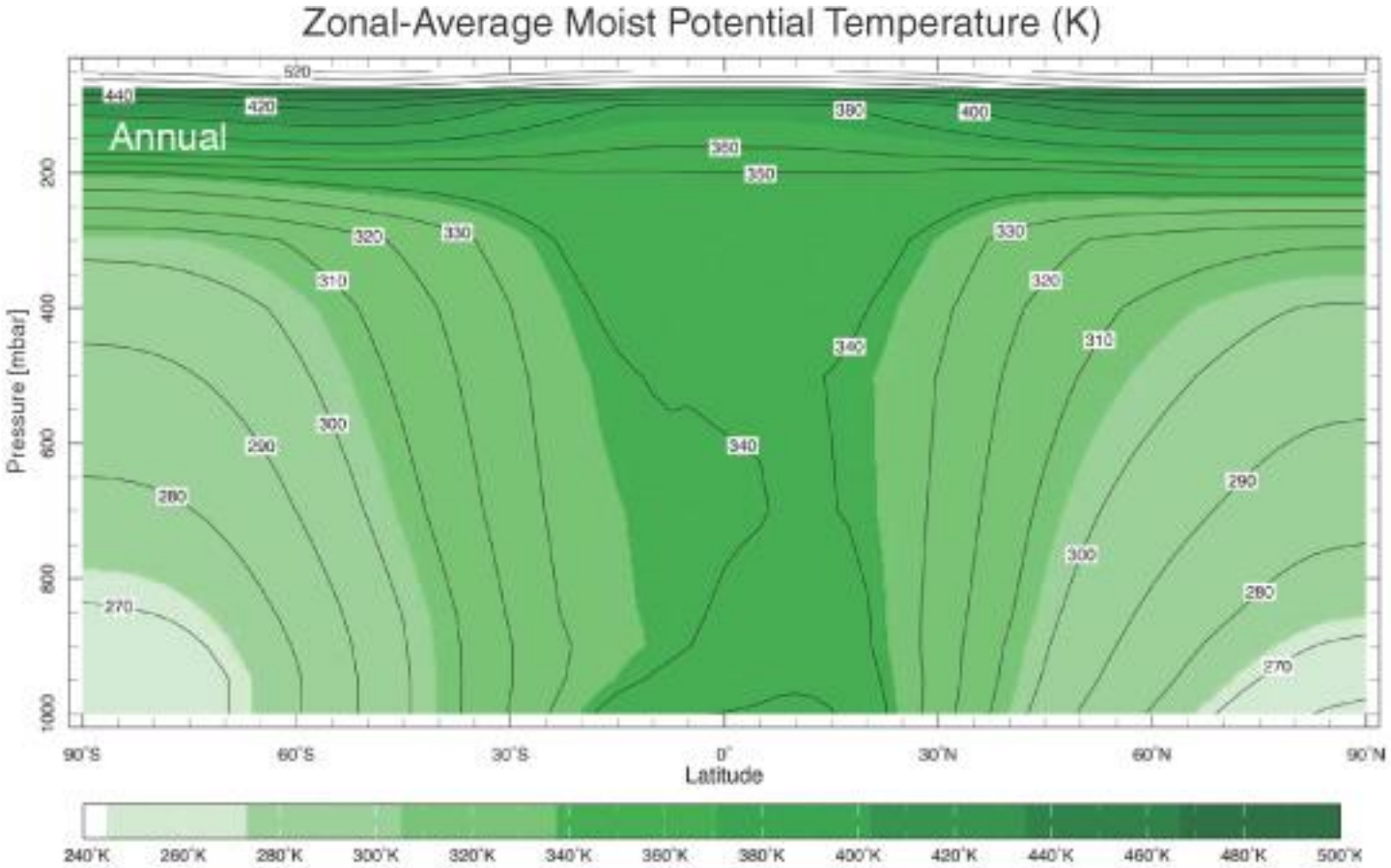

Figure 5.9: The zonal average, annual mean equivalent potential temperature, θ_e, Eq. 4-30.

Temperature in the tropsophere and stratosophere

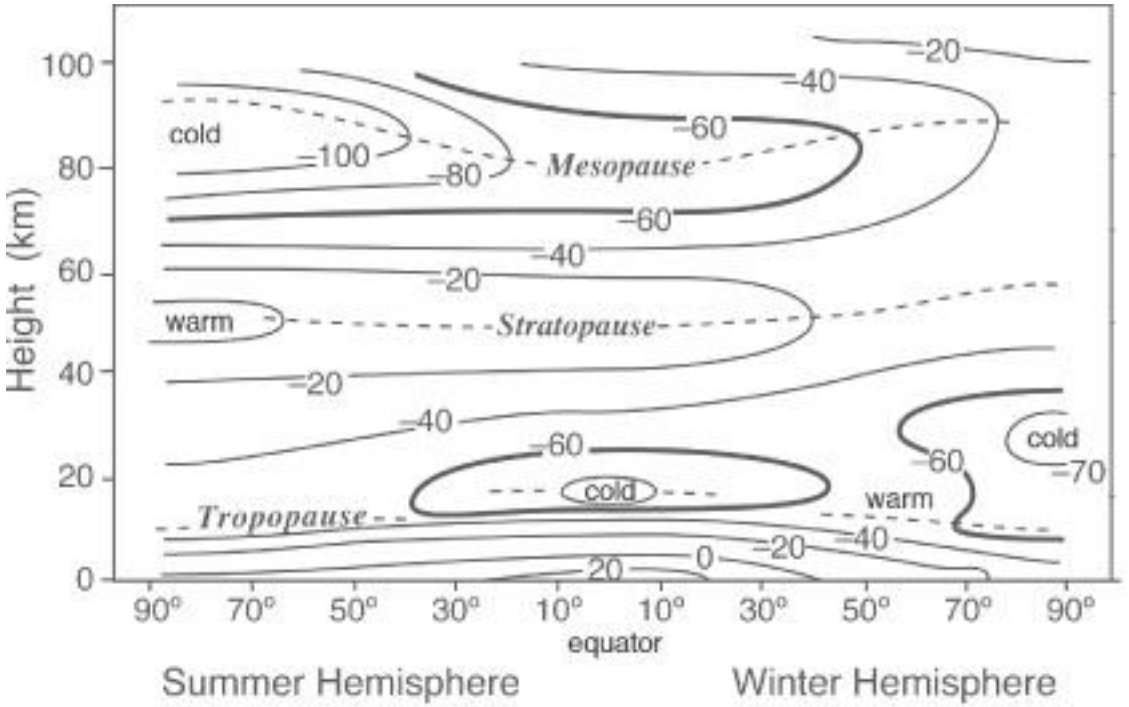

Figure 5.10: The observed, longitudinally averaged temperature distribution (T) at northern summer solstice from the surface to a height of 100 km (after Houghton, 1986). Altitudes at which the vertical T gradient vanishes are marked by the dotted lines and correspond to the demarcations shown on the $T(z)$ profile in Fig. 3.1. The –60°C isopleth is thick. Note the vertical scale is in km compared to Fig. 5.7, which is in pressure. To convert between them, use Eq. 3-8.

Trykk som vertikalkoordinat

Hydrostatisk Likning

$$\frac{\partial p}{\partial z} = -\frac{gp}{RT} \,. \qquad (3\text{-}5)$$

$$\frac{\partial z}{\partial p} = -\frac{RT}{gp}, \qquad (5\text{-}1)$$

Trykk som vertikalkoordinat

Hydrostatisk Likning

$$\frac{\partial p}{\partial z} = -\frac{gp}{RT} \,. \qquad (3\text{-}5)$$

$$\frac{\partial z}{\partial p} = -\frac{RT}{gp}, \qquad (5\text{-}1)$$

or, noting that $p\frac{\partial}{\partial p} = \frac{\partial}{\partial \ln p}$,

$$\frac{\partial z}{\partial \ln p} = -\frac{RT}{g} = -H,$$

Isothermal atmosphere:

T&*H* const with *z* and *p*

z varies as ln*p*

p varies exponentially with *z*

Pressure surfaces (isobarer)

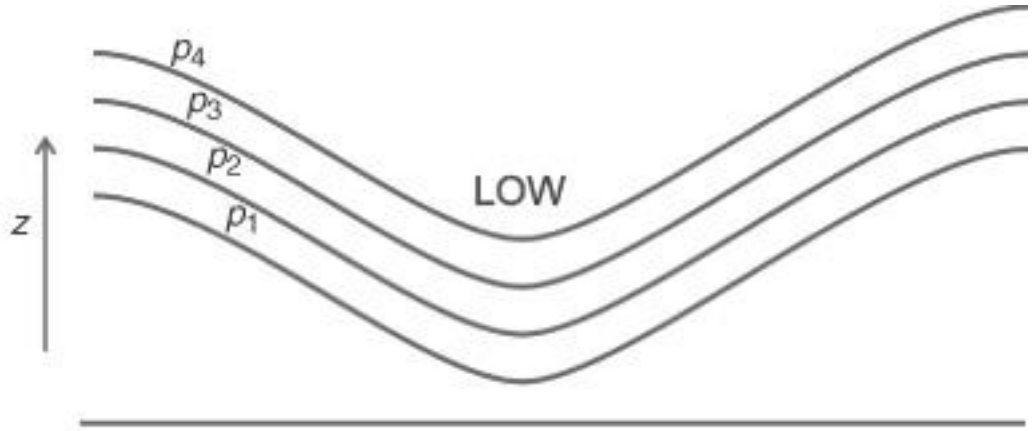

Figure 5.11: The geometry of pressure surfaces (surfaces of constants p_1, p_2, p_3, p_4, where $p_1 > p_2 > p_3 > p_4$) in the vicinity of a horizontal pressure minimum.

Low height
of a pressure surface corresponds to
low pressure

Geopotential height

$$\frac{\partial z}{\partial p} = -\frac{RT}{gp}, \qquad (5\text{-}1)$$

$$z(p) = R\int_{p}^{p_s} \frac{T}{g}\frac{dp}{p}, \qquad (5\text{-}2)$$

where we have set $z(p_s) = 0$

Høyde (fra havets overflate, $p=p_s$) til en trykkflate (p)

Geopotential height high in warm conditions

Pressure surface

Monthly mean

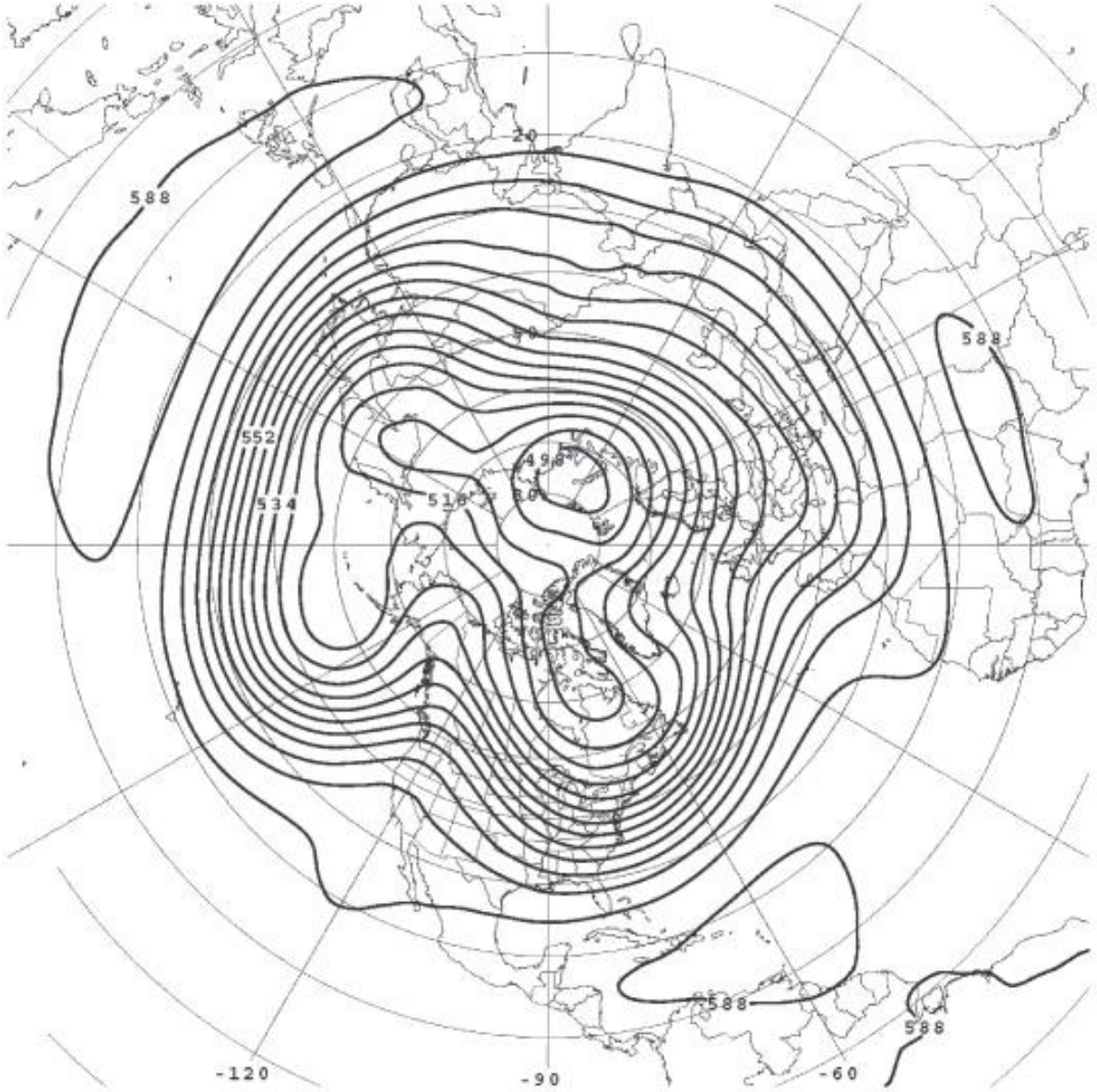

Figure 5.12: The mean height of the 500 mbar surface in January, 2003 (monthly mean). The contour interval is 6 decameters ≡ 60 m. The surface is 5.88 km high in the tropics and 4.98 km high over the pole. Latitude circles are marked every 10°, longitude every 30°.

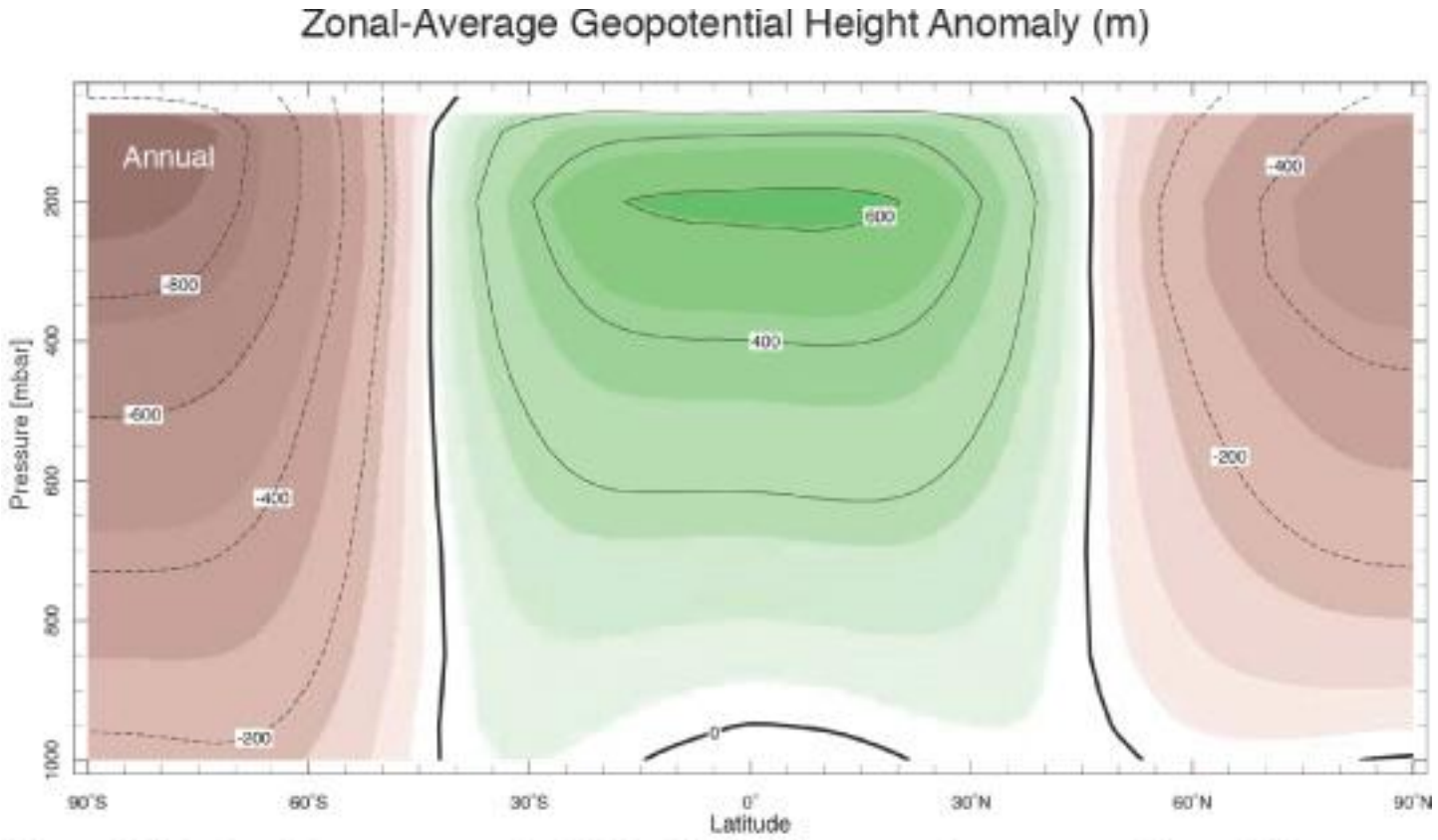

Figure 5.13: Zonal-mean geopotential height (m) for annual mean conditions. Values are departures from a horizontally uniform reference profile.

Thickness of pressure layers

$$z(p) = R \int_{p}^{p_s} \frac{T}{g} \frac{dp}{p}, \qquad (5\text{-}2)$$

Geopotensiell høyde av trykkflaten p

Tykkelsen mellom to trykkflater (p_1 og p_2)

$$z_2 - z_1 = R \int_{p_2}^{p_1} \frac{T}{g} \frac{dp}{p}, \qquad (5\text{-}4)$$

Høy T ➔ Større tykkelse

Tilt of pressure surface

Assume T constant in height but not latitude

$$z = H \ln\left(\frac{p_s}{p}\right).$$

$$H = \frac{RT_0}{g}.$$

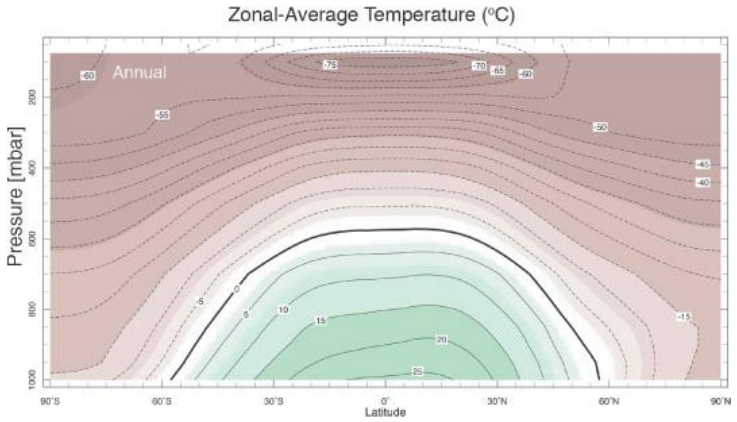

Figure 5.7: The zonally averaged annual-mean temperature in °C.

$$\Delta z_{\text{cold}}^{\text{warm}} = \frac{R\Delta T_{\text{cold}}^{\text{warm}}}{g} \ln\left(\frac{p_s}{p}\right), \qquad (5\text{-}3)$$

For p=500 hPa: ΔT = 40 K → Δz = 811 m

Fig 5.12
Fig 5.13

Tilt of pressure surface

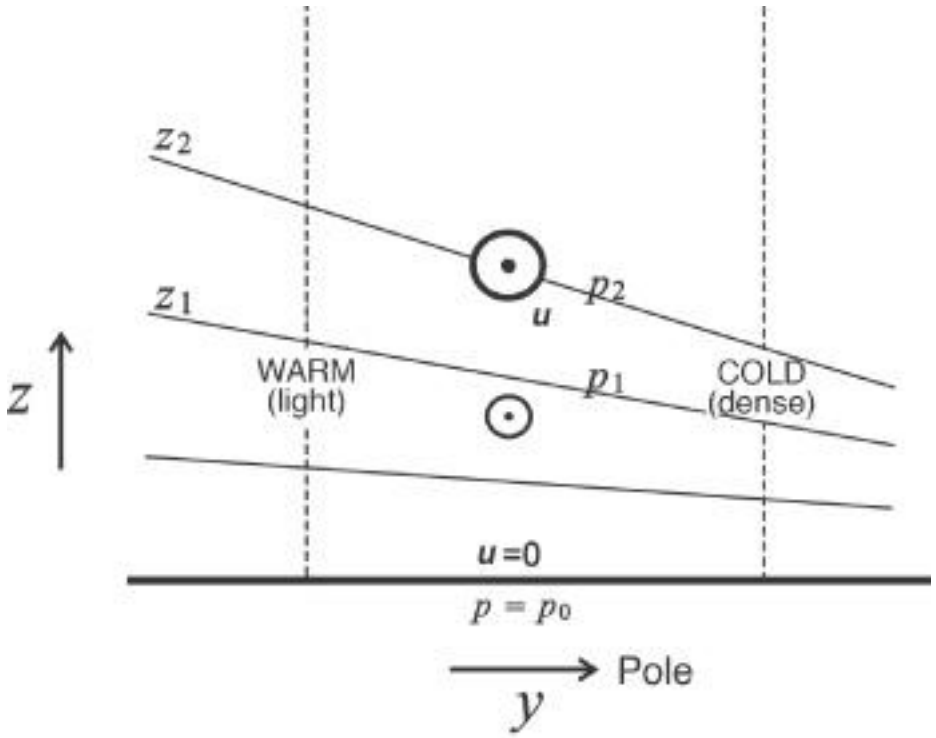

Figure 5.14: Warm columns of air expand, cold columns contract, leading to a tilt of pressure surfaces, a tilt which typically increases with height in the troposphere. In Section 7.3, we will see that the corresponding winds are out of the paper, as marked by *e* in the figure.

Each surface tilting steeper

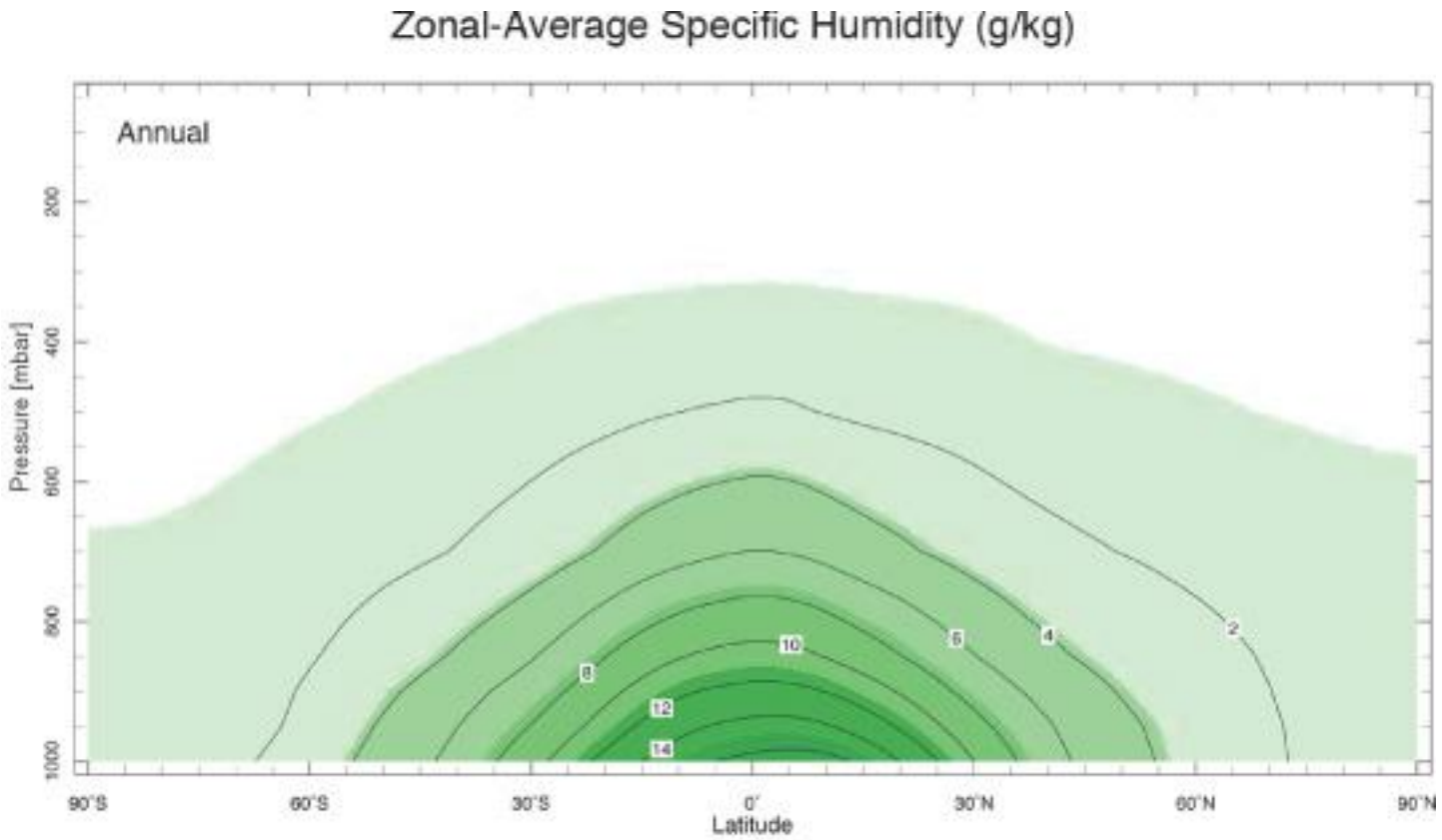

Figure 5.15: Zonally averaged specific humidity q, Eq. 4-23, in g kg^{-1} under annual mean conditions. Note that almost all the water vapor in the atmosphere is found where $T > 0°C$ (see Fig. 5.7).

$$RH(\%) = \frac{q}{q^*} \cdot 100$$

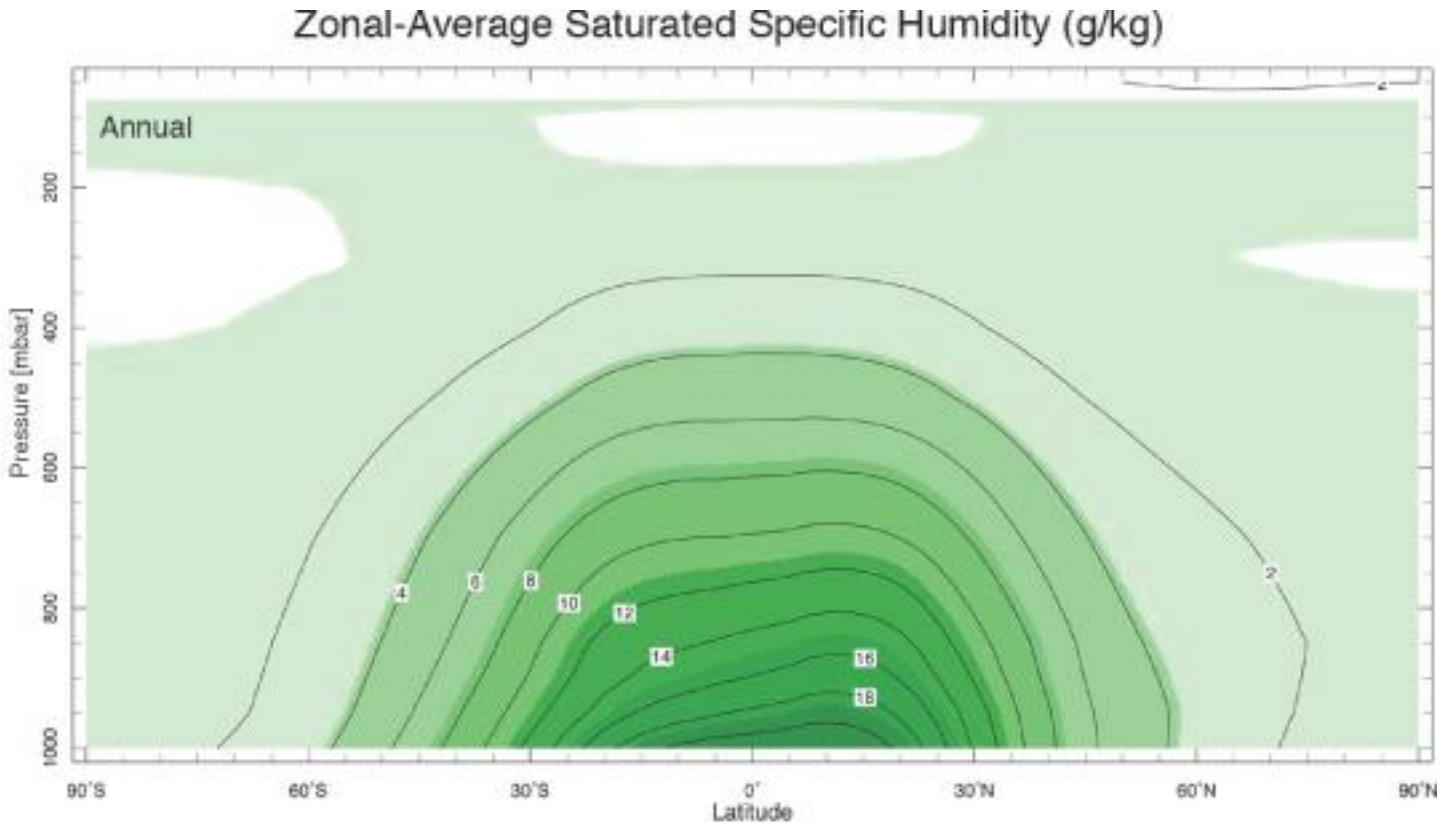

Figure 5.16: Zonally averaged saturated specific humidity, $q*$, in gkg^{-1}, for annual-mean conditions.

$$RH\,(\%) = \frac{q}{q^*} \cdot 100$$

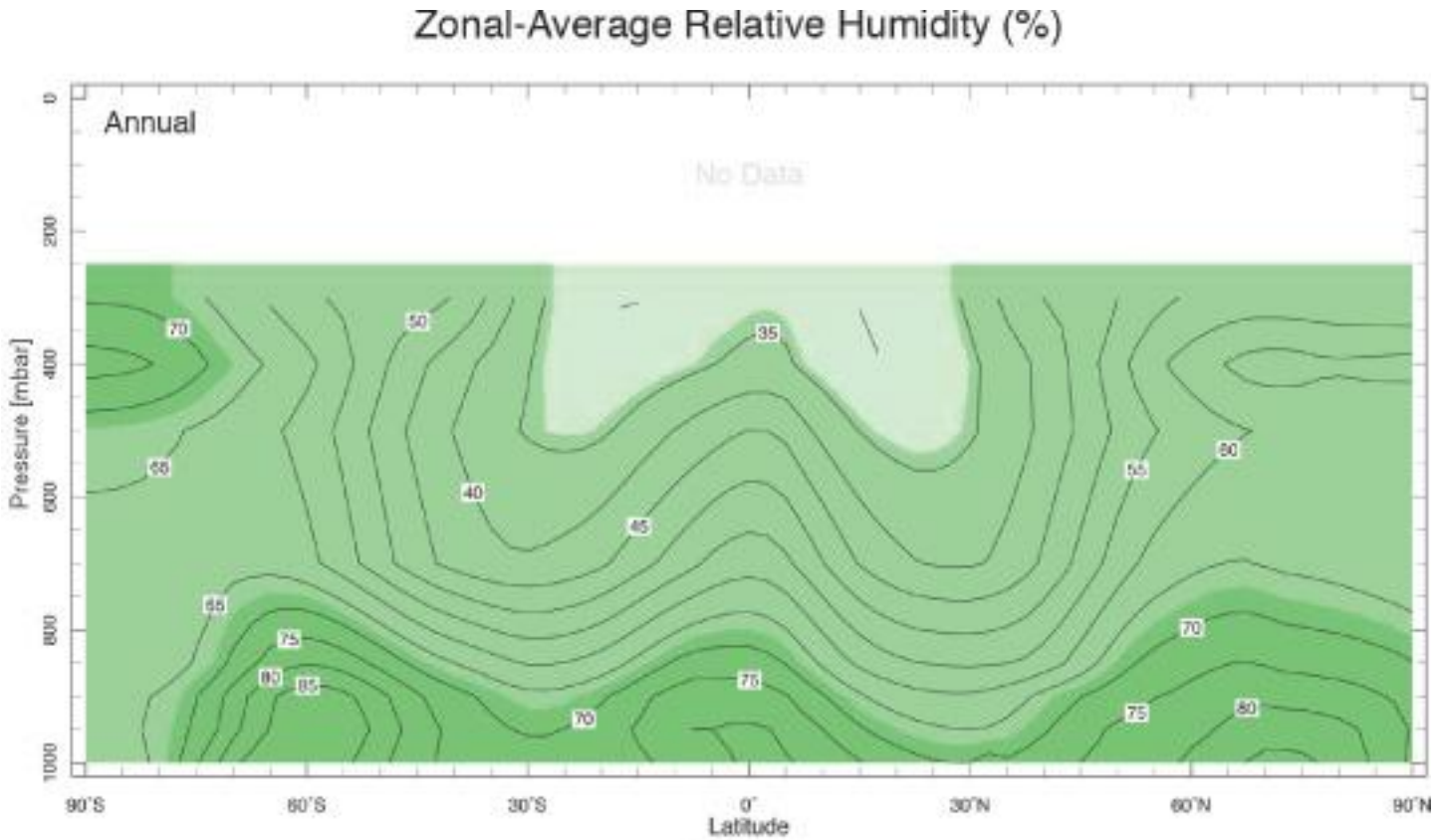

Figure 5.17: Zonal mean relative humidity (%), Eq. 4-25, under annual mean conditions. Note that data are not plotted above 300 mbar, where *q* is so small that it is difficult to measure accurately by routine measurements.

Når luft heves avtar temperaturen og luften kan nå metning. Hvorfor avtar da RH med høyden?

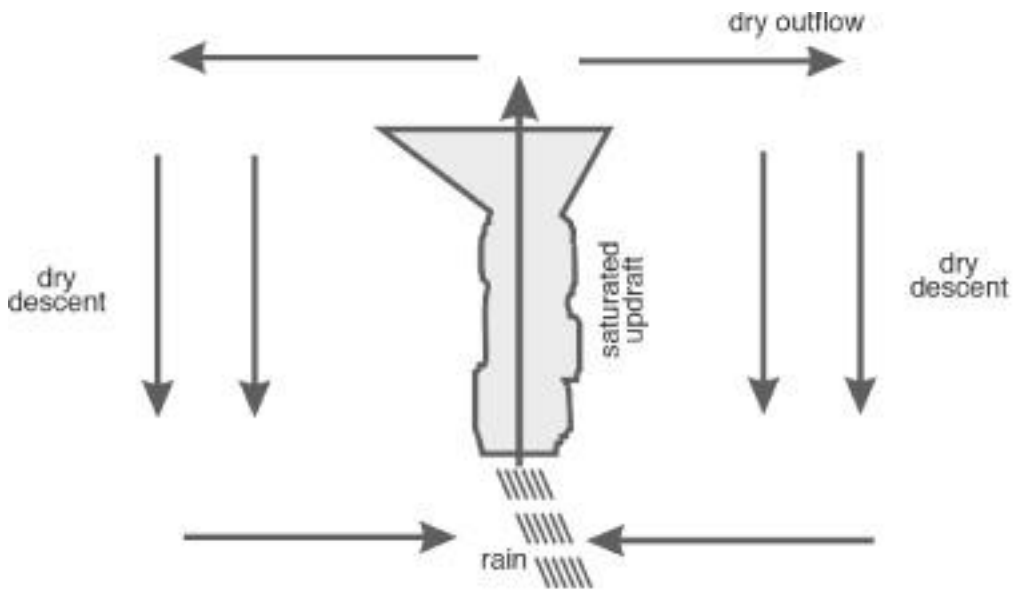

Figure 5.18: Drying due to convection. Within the updraft, air becomes saturated and excess water is rained out. The descending air is very dry. Because the region of ascent is rather narrow and the descent broad, convection acts as a drying agent for the atmosphere as a whole.

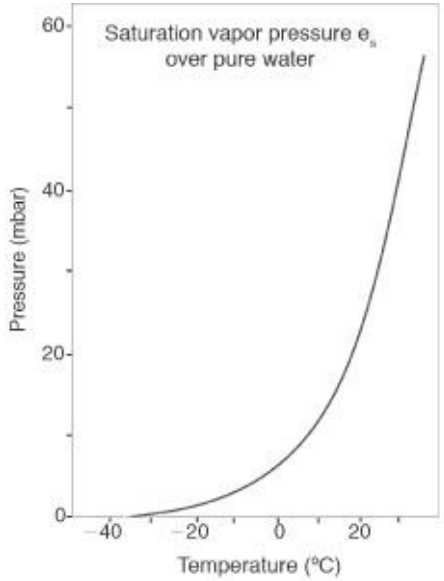

Figure 1.5: Saturation vapor pressure e_s (in mbar) as a function of T in °C (solid curve).

(From Wallace & Hobbs, (2006).)

Arealet med oppdrift er mye mindre en arealet der vi har nedsynkning (subsidens)

Meridional winds
Hadley's suggestion

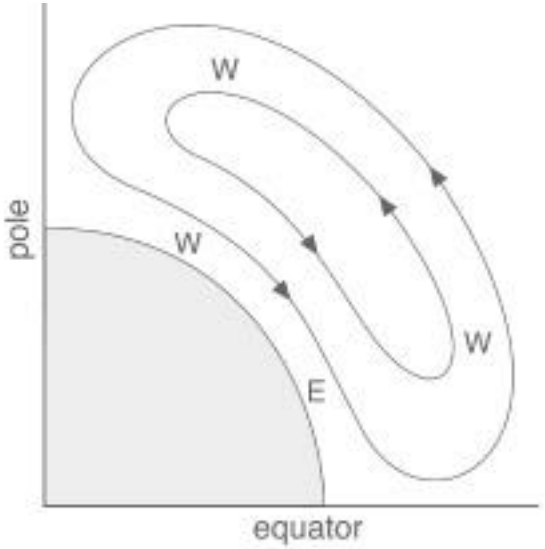

Figure 5.19: The circulation envisaged by Hadley (1735) comprising one giant meridional cell stretching from equator to pole. Regions where Hadley hypothesized westerly (W) and easterly (E) winds are marked.

u: sonal vind (x-retning)
v: meridional vind (y-retning)
w: Vertikal vind (z-retning)

Pressure gradients force winds

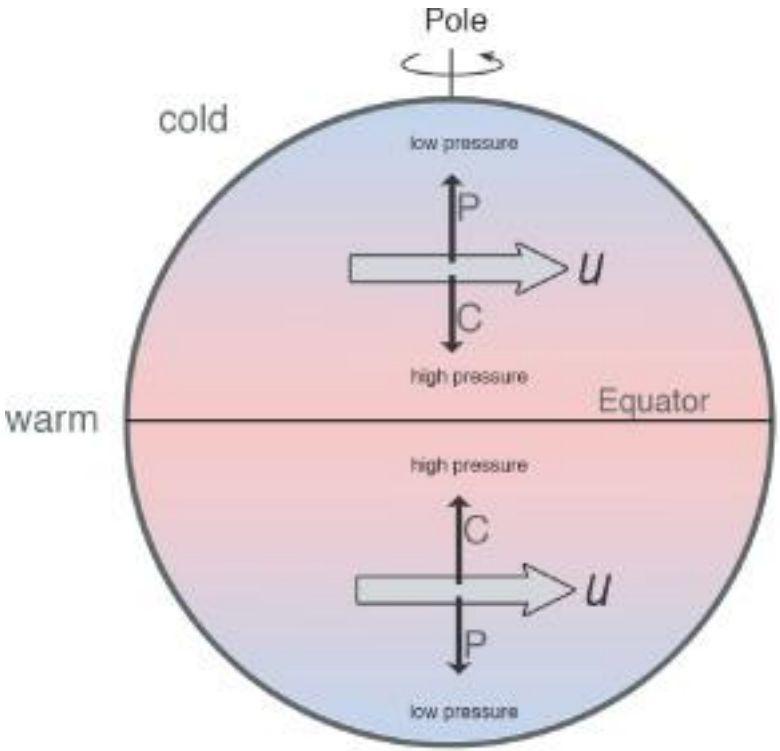

Figure 5.1: The atmosphere is warmer in the equatorial belt than over the polar caps. These horizontal temperature gradients induce, by hydrostatic balance, a horizontal pressure gradient force "P" that drive rings of air poleward. Conservation of angular momentum induces the rings to accelerate eastwards until Coriolis forces acting on them, "C," are suffcient to balance the pressure gradient force "P," as discussed in Chapters 6 and 7.

Zonal winds

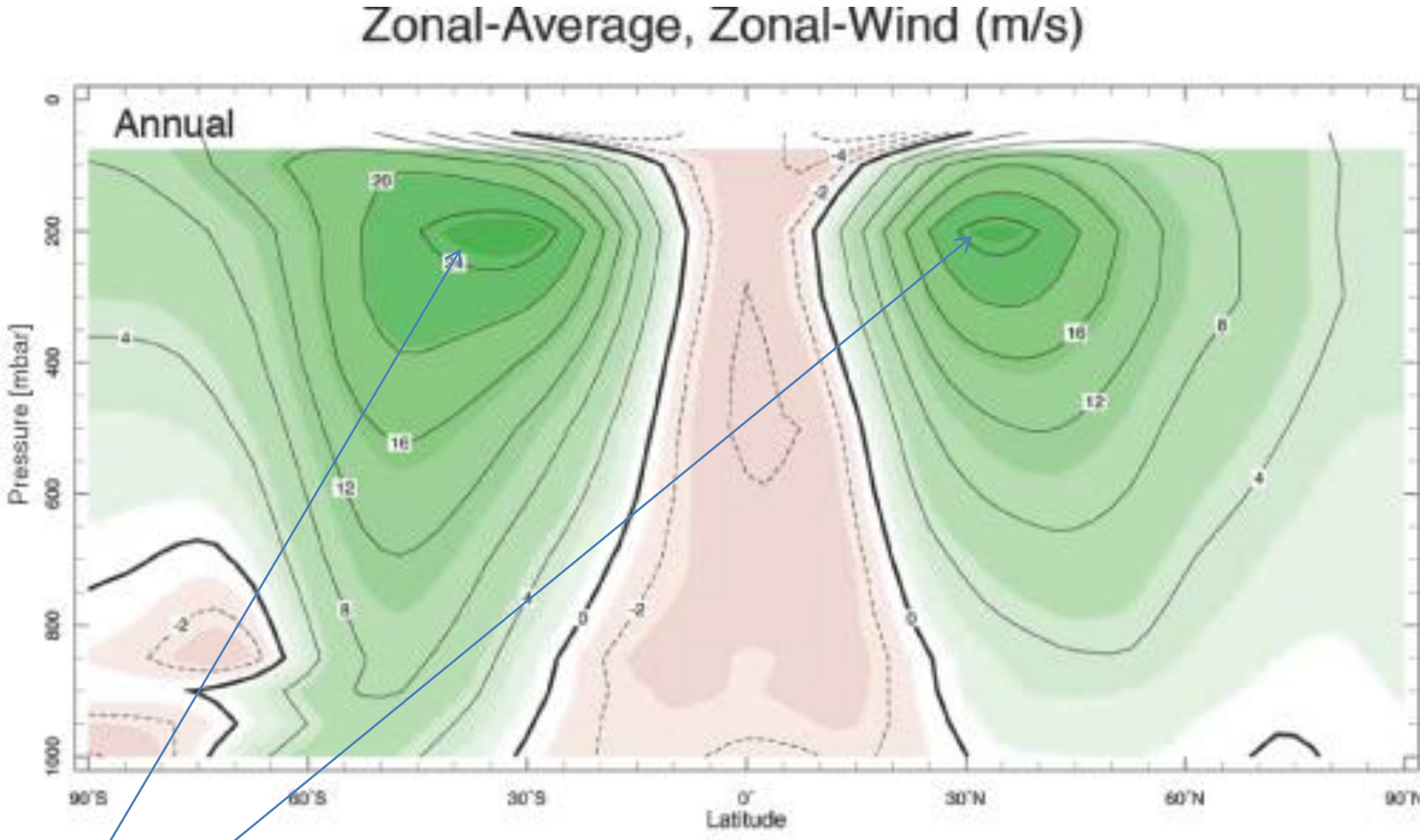

Sub-tropiske jetstrømmer (fra vest mot øst)

Zonal winds

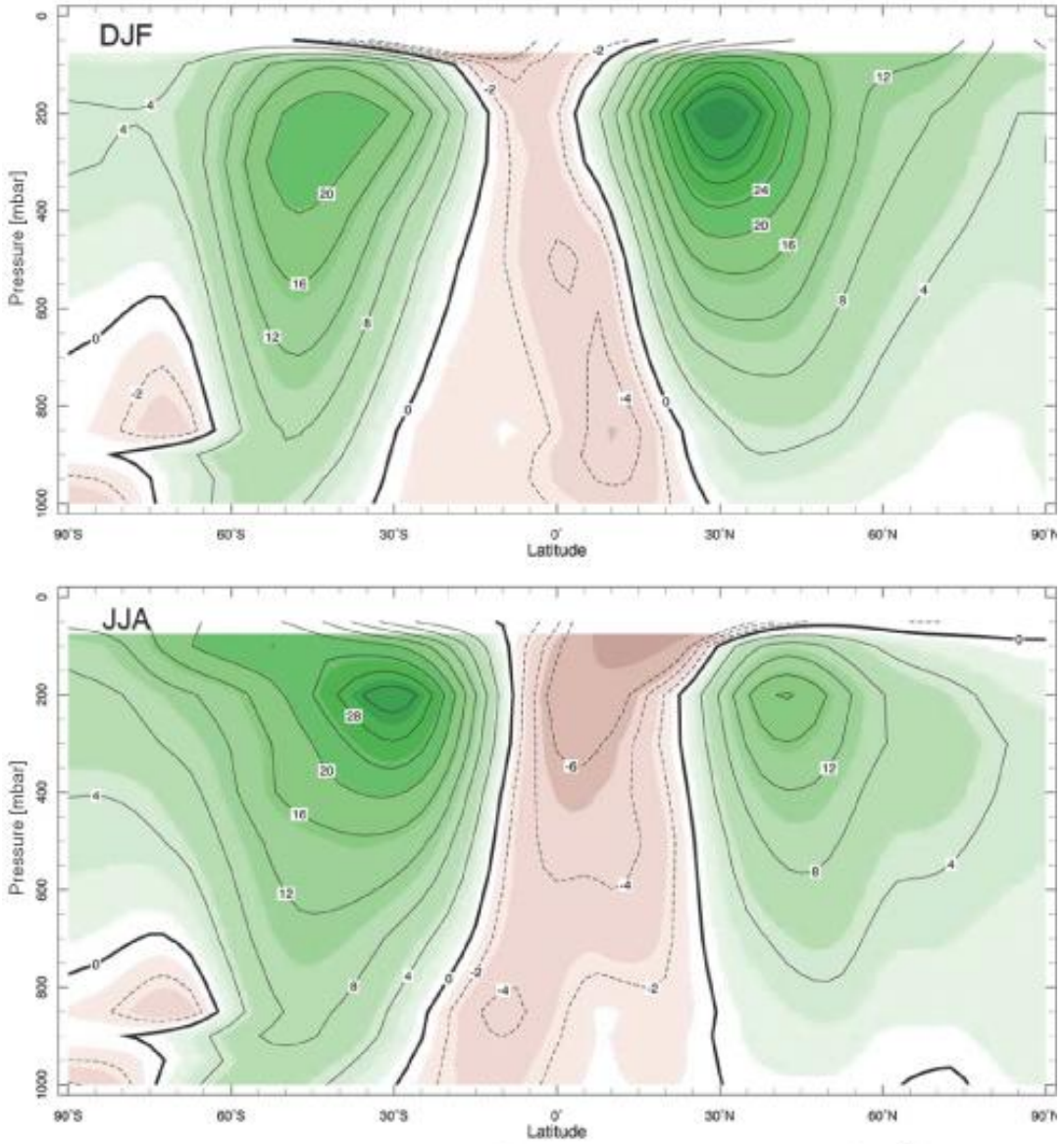

Figure 5.20: Meridional cross-section of zonal-average zonal wind (ms^{-1}) under annual mean conditions (top), DJF (December, January, February) (middle) and JJA (June, July, August) (bottom) conditions.

Meridional winds, gitt ved en strømfunksjon

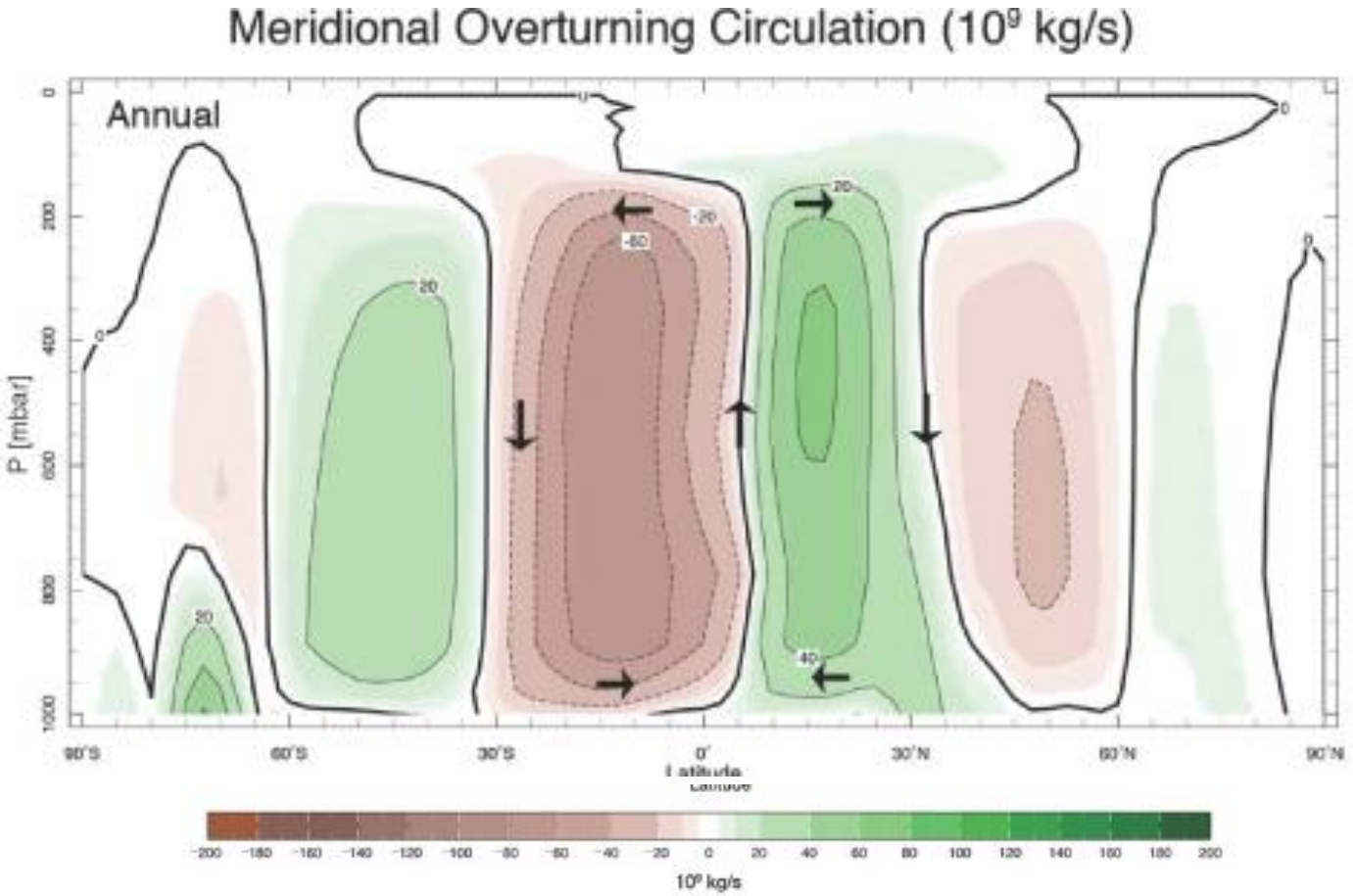

Figure 5.21: The meridional overturning streamfunctio χ of the atmosphere in annual mean, DJF, and JJA conditions. [The meridional velocities are related to χ by $v = -(\rho a \cos\varphi)^{-1} \partial\chi / \partial z$; $w = (\rho a^2 \cos\varphi)^{-1} \partial\chi / \partial\varphi$ Units are in 10^9 kg s^{-1}, or Sverdrups, as discussed in Section 11.5.2. Flow circulates around positive (negative) centers in a clockwise (anticlockwise) sense. Thus in the annual mean, air rises just north of the equator and sinks around ±30°.

Meridional winds

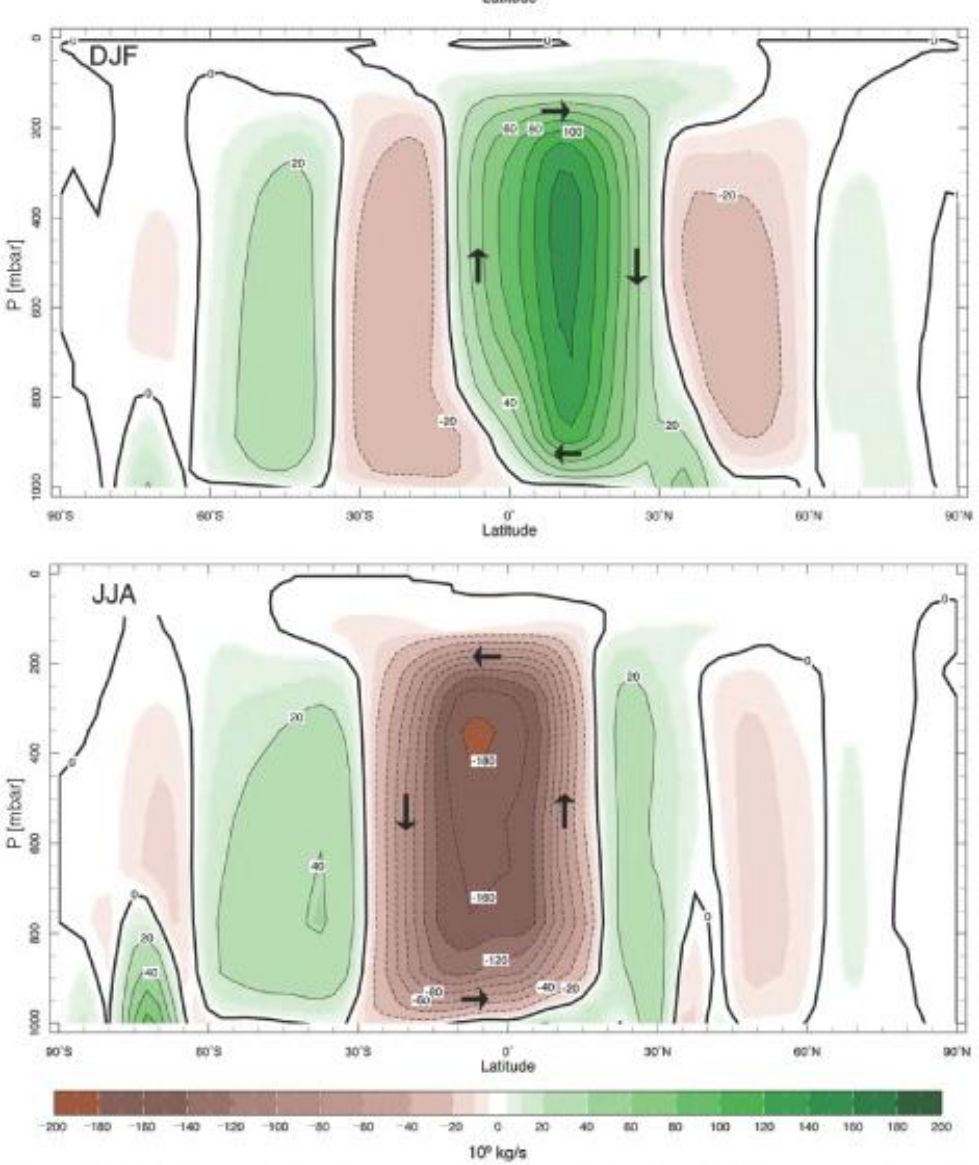

Figure 5.21: The meridional overturning streamfunction ? of the atmosphere in annual mean, DJF, and JJA conditions. [The meridional velocities are related to χ by $v = -(\rho a \cos\varphi)^{-1} \partial\chi / \partial z$; $w = (\rho a^2 \cos\varphi)^{-1} \partial\chi / \partial\varphi$ Units are in 10^9 kg s^{-1}, or Sverdrups, as discussed in Section 11.5.2. Flow circulates around positive (negative) centers in a clockwise (anticlockwise) sense. Thus in the annual mean, air rises just north of the equator and sinks around ±30°.

Geopotential height map

Monthly mean

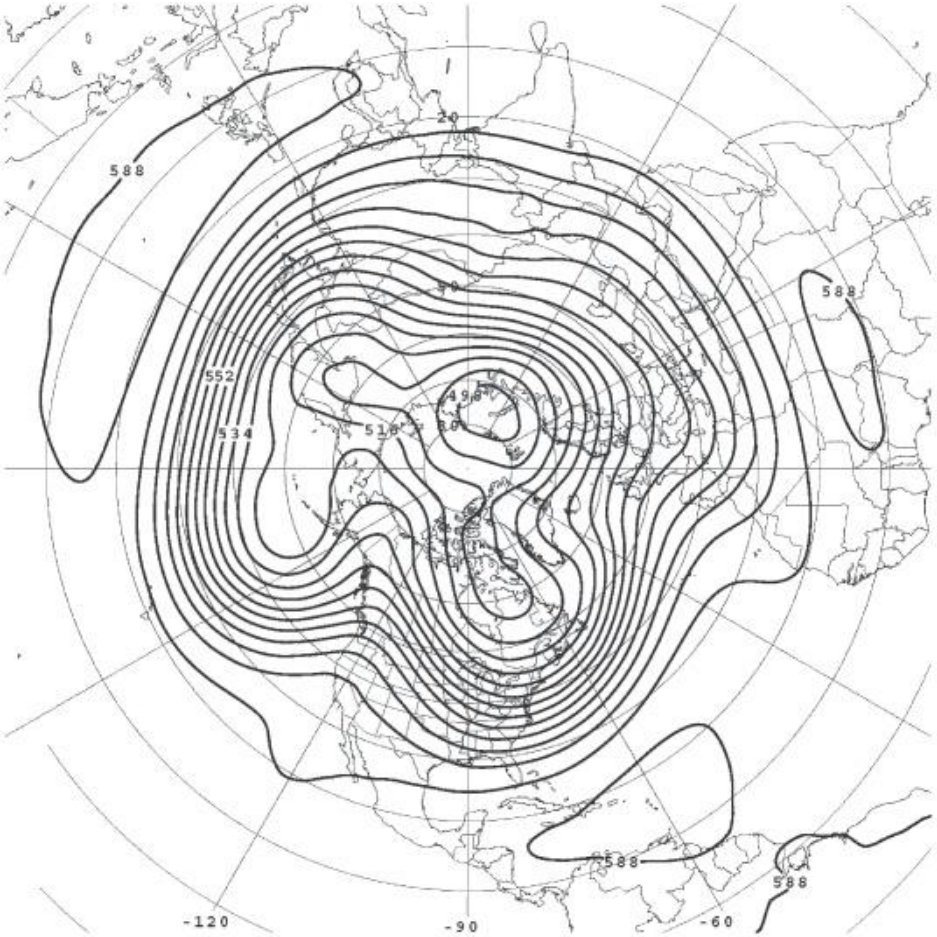

Figure 5.12: The mean height of the 500 mbar surface in January, 2003 (monthly mean). The contour interval is 6 decameters ≡ 60 m. The surface is 5.88 km high in the tropics and 4.98 km high over the pole. Latitude circles are marked every 10°, longitude every 30°.

Snapshot

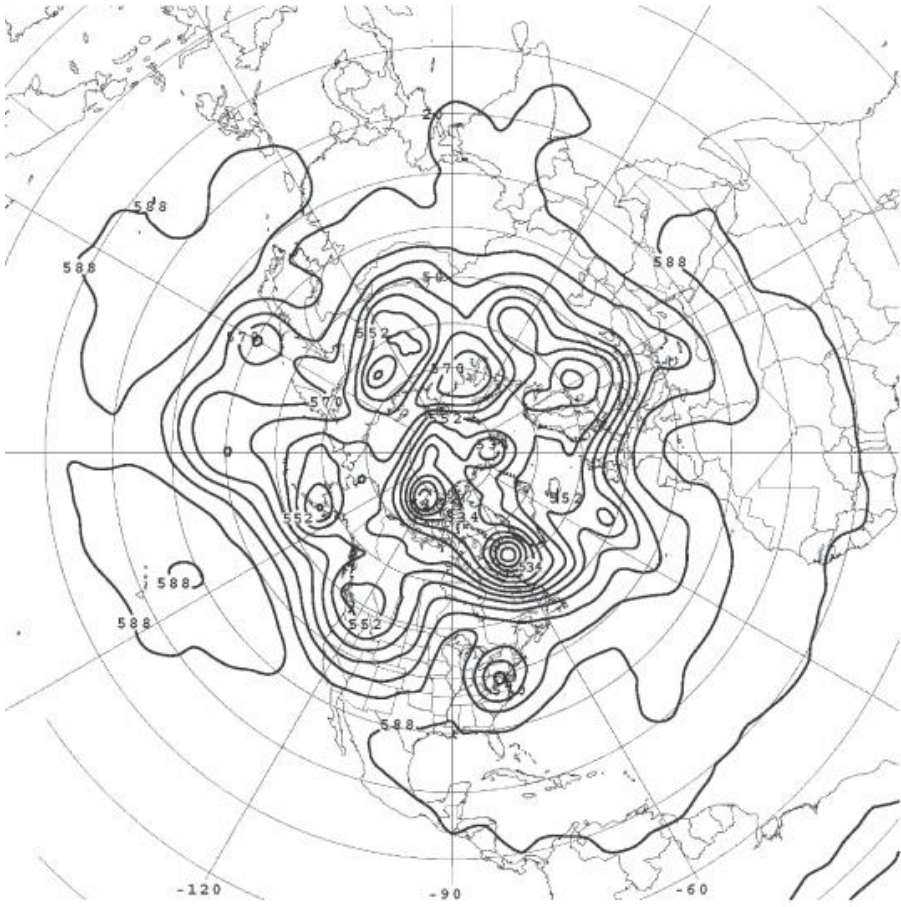

Figure 5.22: Typical 500 mbar height analysis: the height of the 500 mbar surface (in decameters) at 12 GMT on June 21, 2003. The contour interval is 6 decameters = 60 m. The minimum height is 516 decameters and occurs in the intense lows over the pole.

Snapshot

Eddies

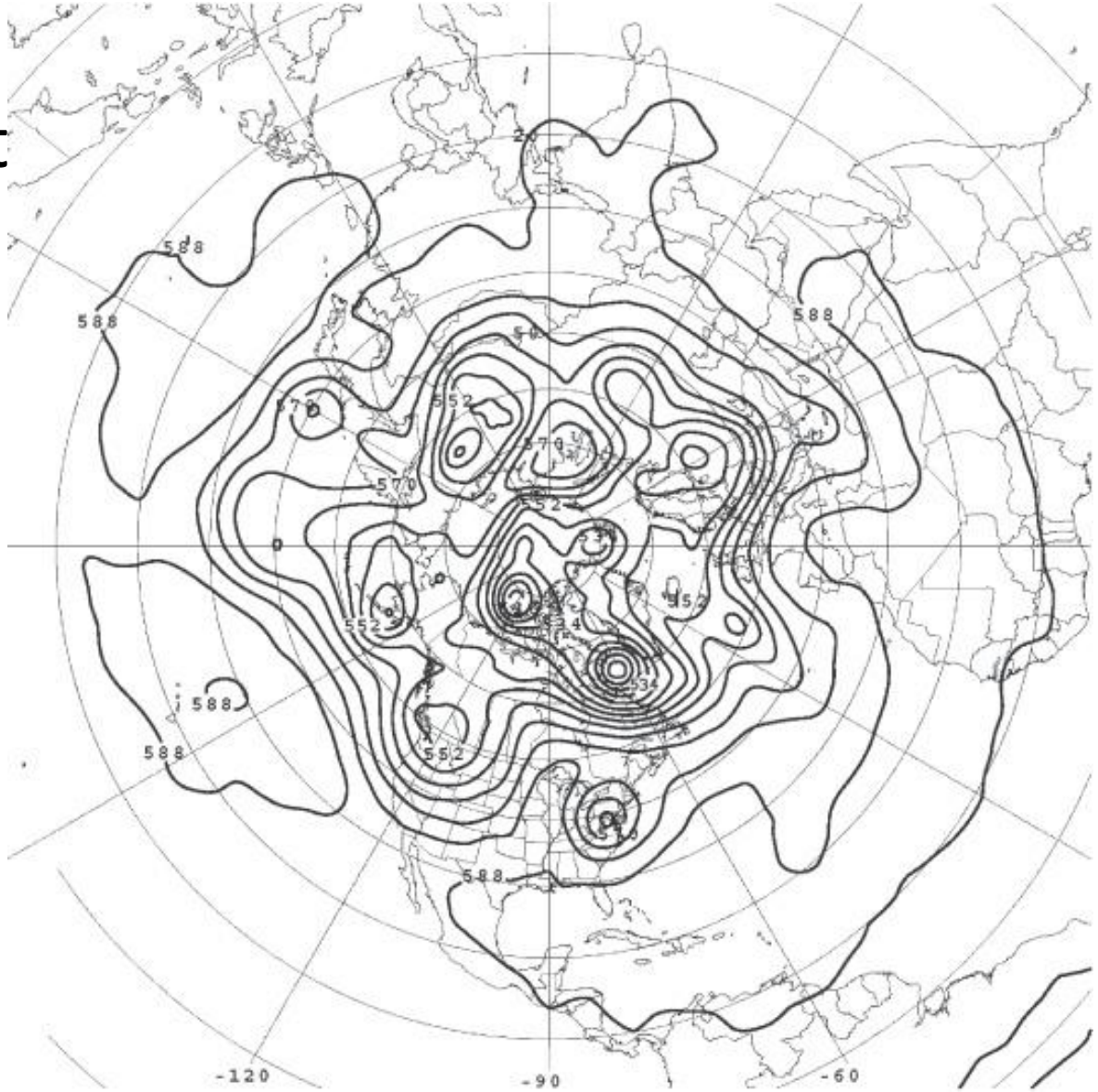

Figure 5.22: Typical 500 mbar height analysis: the height of the 500 mbar surface (in decameters) at 12 GMT on June 21, 2003. The contour interval is 6 decameters = 60 m. The minimum height is 516 decameters and occurs in the intense lows over the pole.

Monday 05 September 2016 1200 UTC ECMWF t+0 VT: Monday 05 September 2016 1200 UTC
850 hPa Temperature/500 hPa Geopotential